Impulsive control strategies of mRNA and protein dynamics on fractional-order genetic regulatory networks with actuator saturation and its oscillations in repressilator model

Article *in* Biomedical Signal Processing and Control · April 2023

DOI: 10.1016/j.bspc.2023.104576

CITATION
1

READS
83

5 authors, including:

Govindasamy Narayanan
Kunsan National University
19 PUBLICATIONS **412** CITATIONS
SEE PROFILE

M. Syed Ali
Thiruvalluvar University
195 PUBLICATIONS **3,949** CITATIONS
SEE PROFILE

Karthikeyan Rajagopal
Chennai Institute Of Technology
395 PUBLICATIONS **6,444** CITATIONS
SEE PROFILE

Anuwat Jirawattanapanit
Phuket Rajabhat University
22 PUBLICATIONS **37** CITATIONS
SEE PROFILE

Biomedical Signal Processing and Control 82 (2023) 104576

Contents lists available at ScienceDirect

Biomedical Signal Processing and Control

journal homepage: www.elsevier.com/locate/bspc

Impulsive control strategies of mRNA and protein dynamics on fractional-order genetic regulatory networks with actuator saturation and its oscillations in repressilator model

G. Narayanan [a], M. Syed Ali [b], Rajagopal Karthikeyan [c], Grienggrai Rajchakit [d,*], Anuwat Jirawattanapanit [e]

[a] Center for Computational modeling, Chennai Institute of Technology, Chennai 600069, India
[b] Complex Systems and Networked Science Laboratory, Department of Mathematics, Thiruvalluvar University, Vellore 632 115, Tamilnadu, India
[c] Center for Nonlinear Systems, Chennai Institute of Technology, Chennai 600069, India
[d] Department of Mathematics, Faculty of Science, Maejo University, Chiang Mai 50290, Thailand
[e] Department of Mathematics, Faculty of Science, Phuket Rajabhat University (PKRU), Phuket 83000, Thailand

ARTICLE INFO

Keywords:
Genetic regulatory networks
Fractional-order
Impulsive control
Actuator saturation
Repressilator model

ABSTRACT

In genetic regulatory networks (GRNs), the control strategies of messenger RNA (mRNA) and protein play a key role in regulatory mechanisms of gene expression, especially in translation and transcription. However, the influence of impulsive control strategies on oscillatory gene expression is not well understood. In this article, by considering the impulsive control strategies of mRNA and protein, a novel fractional-order genetic regulatory networks with actuator saturation is proposed. By applying polytopic representation technique, the actuator saturation term is first considered into the design of impulsive controller, and less conservative linear matrix inequalities (LMIs) criteria that guarantee finite-time Mittag-Leffler stabilization problem for fractional-order genetic regulatory networks are given. The derived sufficient conditions can easily be verified by designing impulsive control gains and solving simple LMIs. Finally, to investigate the effectiveness and applicability of the control strategies, an interesting simulation example as a synthetic oscillatory network of transcriptional regulators in Escherichia coli is illustrated.

1. Introduction

Genetic regulatory networks (GRNs) are biochemical networks that regulate gene expression and perform complex biological functions (via direct or indirect interactions between deoxyribonucleic acid (DNA), ribonucleic acid (RNA), proteins, and small molecules) as shown in Fig. 1. GRNs are a significant topic in bioscience and biomedical engineering, as they can help many biologists, engineers, and scientists understand a variety of complex challenges in living cells [1–3]. Because many traits and diseases are linked to dysfunctional transcriptional regulators or mutations in regulatory sequences, understanding gene expression regulation has an immediate impact on biology and medicine. Acquiring precise information about the states of GRNs is particularly useful in biological and biomedical sciences for applications such as gene identification and medical diagnosis/treatment [4,5]. One of the key challenges in this area is to (i) understand the cells behavior and control their operations; and (ii) discover how cellular systems fail in disease. Mathematical modeling and simulation tools aid in understanding how complex GRNs, which are made up of numerous genes and their tangled interactions, control the functioning of living systems. Understanding the dynamics and predicting the behavior of GRNs is critical in cell and molecular biology, namely different GRNs models have been developed. Hence, the research on GRNs includes the following aspects: gene circuit control design [6], modeling [7], and stability analysis [8]. Stability analysis is one of the most noticeable aspects of many dynamic systems, including GRNs. Various researchers have dedicated their efforts to the stability mechanism and biological rhythms, and both theoretical analysis and biotic experiments have contributed a huge quantity of beneficial research results. In [9], a simple gene circuit consisting of the regulator and transcriptional repressor modules in Escherichia coli was built, and the stability gain produced by negative feedback was demonstrated. It has been widely researched that time delay is an unavoidable factor in modeling, designing, and controlling GRNs because they naturally occur as a result of

* Corresponding author.
E-mail addresses: narayanang@citchennai.net (G. Narayanan), syedgru@gmail.com (M. Syed Ali), rkarthiekeyan@gmail.com (R. Karthikeyan), kreangkri@mju.ac.th (G. Rajchakit), anuwat.j@pkru.ac.th (A. Jirawattanapanit).

https://doi.org/10.1016/j.bspc.2023.104576
Received 26 July 2022; Received in revised form 12 December 2022; Accepted 9 January 2023
Available online 17 January 2023

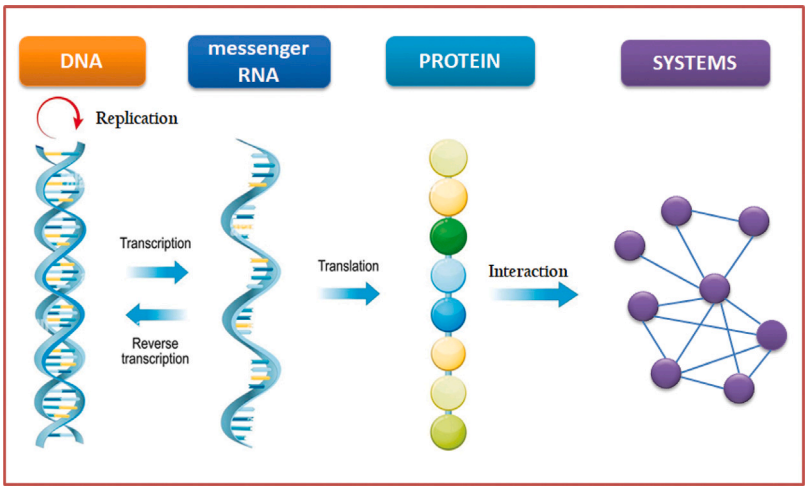

Fig. 1. Gene regulatory network mechanism.

transcription, transcript splicing, processing, and protein synthesis [10–16]. Therefore, the biological scopes of GRNs, it is of great significance to study the dynamic behavior of messenger RNA (mRNA) and protein in regulatory mechanisms with time-varying delays.

The involvement of memory and hereditary properties in dealing with fractional-order derivatives provides a more realistic way to biological models [17]. Because of the memory effect, non-integer models incorporate all previous information from the past, allowing them to more accurately predict and translate molecular models [18]. Fractional-order genetic regulatory networks (FGRNs) have two advantages over integer-order GRNs: more degrees of freedom and infinite memory [19–21]. Furthermore, experiments on yeast cell cycle gene expression data show that the proposed mathematical model is better suited to modeling genetic regulatory mechanisms. Although fractional-order differential equations have been used to GRNs model due to their lower data fitting error on test data than integer-order models, few articles have been published on FGRNs. Therefore, FGRNs have formulated numerous molecular models of fractional derivative to study the transmission dynamics during the past few years [22,23]. All the results above have shown that FGRNs are of great importance in enlightening the mechanism of multistability and biological rhythms.

In recent decades, the impulsive control approach has been intensively researched and applied to the analysis of nonlinear system dynamics [24–26]. In some practical applications, impulsive control is really valuable, such as biological models [27], multi-agent systems [28], neural networks [29], and so on. Because it has some excellent characteristics, impulsive control has recently received a lot of attention [30]. It is reasonable and powerful to introduce the ideas and methods from system and control theory to underly the complicated biological functions of living organisms in their entirety [31–34]. Environmental cues, differentiation cues, and disease all cause regulatory circuits controlling gene expression to constantly rewire [35]. GRN states are frequently impulsively changed in response to transient environmental stimuli. Indeed, the gene regulatory mechanism is always exposed to intrinsic noise caused by the random births and deaths of individual molecules, as well as extrinsic noise caused by environmental variations. Because environmental noises can affect the stability of equilibrium states, it is critical to investigate impulsive generalizations of the GRNs in which the states of the models are abruptly changed [36]. Few authors have developed impulsive control strategies to investigate the stability issue of GRNs models to date [37,38]. Although more and more experts recognize the significance of actuator saturation, the findings of saturated impulsive control are extremely rare. This is because it is very challenging to deal with saturation nonlinearity and the estimate of domain of attraction. The authors [39] investigated the impact of saturation on network performance. Actuator saturation can degrade dynamic performance and even destabilize the system under study. An impulse saturation can have a significant impact on system dynamics [40–42]. However, despite its practical significance, the finite-time Mittag-Leffler stabilization (FTMLS) problem for FGRNs via impulsive control with actuator saturation has not been investigated yet.

Inspired by above, this article addresses the finite-time Mittag-Leffler stabilization problem of fractional-order genetic regulatory networks via impulsive control with actuator saturation. The main contributions are:

(1) A novel the controller that involves saturated impulsive control has been designed to achieve FTMLS problem of FGRNs for the first time in this article.
(2) The sufficient criteria that ensure the FTMLS of the proposed FGRNs are determined using the novel Lyapunov functional, and the proposed conditions are represented in terms of solvable LMIs.
(3) Furthermore, we take advantage of how polytopic representation approaches handle saturation nonlinearity.
(4) Finally, to illustrate and demonstrate the efficiency of our obtained results, we present some new simulation results that reveal the time responses of the state variables with and without the inclusion of impulsive actuator saturation into the repressilator model.

To better illustrate the biological scopes of GRNs and major contributions of theoretical as well as practical significance of this article, we provide Table 1 for comparison with other research works on GRNs, where fractional-order, impulsive control, impulsive actuator saturation, linear matrix inequalities (LMIs), finite-time Mittag-Leffler stabilization (FTMLS), and repressilator model. Moreover, $\surd$ means this item is included in that paper, $\times$ means it is not.

Notation: The notes of the symbols appearing in the article is as follows: $\mathcal{C}$ the complex numbers; $\mathcal{R}$ the real numbers; $\mathcal{R}_+$ the real numbers; $\mathcal{Z}_+$ the positive integers. $\mathcal{C}^q$ and $\mathcal{R}^q$ denotes the set of all q-dimensional complex-valued vectors and real-valued vectors, respectively. $\mathcal{R}^{m\times m}$ denotes the set of all $m\times m$ real matrices. diag$\{\cdots\}$ is a block diagonal matrix. $\mathcal{I}_n$ stands for the n × n identity matrix. ${}_{t_0}^{\mathbb{C}}D_t^{\gamma}$ a denotes the Caputo fractional derivative with order γ. $\mathbf{E}_{\gamma}(\cdot)$ denotes the Mittag-Leffler function of $(\cdot)$. For a real matrix Ω, Ω^T stands for its transpose, and $\lambda_{\max}(\Omega)$. $\lambda_{\min}(\Omega)$ are maximum and minimum eigenvalues of Ω respectively. The saturation function $\mathbf{sat}(\hbar(t)) = (\mathbf{sat}(\hbar_1(t)), \mathbf{sat}(\hbar_2(t)), \ldots, \mathbf{sat}(\hbar_q(t)))^T$ with $\mathbf{sat}(\hbar_1(t)) = sign(h_1(t))\min\{\hbar_{0\tau}, |\hbar_\tau(t)|\}$ $(\tau \in \mathcal{M})$, where $\hbar_{0\tau} \in \mathcal{R}_+$ is the τ^{th} element

Table 1
Comparison with existing works.

GRNs	[8–15]	[3,7]	[11,14]	[18–21]	[22]	[23,36]	[37,38]	This article
Fractional-order	×	√	×	√	√	√	×	√
Impulsive control	×	×	×	×	×	√	√	√
Impulsive actuator saturation	×	×	×	×	×	×	×	√
LMIs	√	√	√	×	×	×	√	√
FTMLS	×	×	×	×	×	×	×	√
Repressilator model	×	×	√	√	×	×	×	√

of the vector $\hbar_0 \in \mathcal{R}_+^q$ and is the know saturation level. $\mathbf{co}\{\nu\}$ represents the convex hull defined by the vertices ν. Let $\mathfrak{R} = \{\mathfrak{R}_\jmath : \jmath \in \Lambda\}$ be the set of $\jmath \times \jmath$ diagonal matrices whose diagonal element take value 1 or 0. The notation $*$ is used to denote the symmetric term in a matrix

2. Problem description and preliminaries

In this section, some basic definitions of fractional calculus, assumptions, and lemmas are given, and the finite-time Mittag-Leffler stabilization problem description of fractional-order genetic regulatory networks with the time-varying delays model is presented.

Definition 2.1 ([18]). For any $t \geq t_0$, the fractional integral for a function $\mathfrak{F}(t)$ is given by

$$ {}_{t_0}D_t^{-\gamma}\mathfrak{F}(t) = \frac{1}{\Gamma(\gamma)}\int_{t_0}^{t}(t-\xi)^{\gamma-1}\mathfrak{F}(\xi)d\xi, \quad t \geq t_0. \tag{1} $$

The Caputo derivative for a function $\mathfrak{F}(t) \in C^q([t_0, t], \mathcal{R}^q)$ is defined by

$$ {}_{t_0}^{\mathbb{C}}D_t^{\gamma}\mathfrak{F}(t) = \begin{cases} \frac{1}{\Gamma(q-\gamma)}\int_{t_0}^{t}\frac{\mathfrak{F}^{(q)}(\xi)}{(t-\xi)^{\gamma+1-q}}d\xi, & q-1<\gamma<q, \\ \frac{d^q}{dt^q}\mathfrak{F}(t), & \gamma = q. \end{cases} \tag{2} $$

In particular, for $\gamma \in (0,1)$ then ${}_{t_0}^{\mathbb{C}}D_t^{\gamma}\mathfrak{F}(t) = (1/\Gamma(1-\gamma))\int_{t_0}^{t}(\mathfrak{F}'(\xi)/(t-\xi)^{\gamma})$.

Definition 2.2 ([29]). The Mittag-Leffler function (two parameter type) can be expressed as

$$ \mathbf{E}_{\gamma,\tau}(z) = \sum_{k=0}^{\infty}\frac{z^k}{\Gamma(k\gamma+\tau)}, $$

where $z \in C$, $\gamma > 0$ and $\tau > 0$. If τ=1, the Mittag-Leffler function (one parameter type) can be expressed as

$$ \mathbf{E}_{\gamma}(z) = \sum_{k=0}^{\infty}\frac{z^k}{\Gamma(k\gamma+1)} = E_{\gamma,1}(z). $$

We consider a class of fractional-order genetic regulatory networks with time-varying delays as follows [22,23]:

$$ \begin{cases} {}_{0}^{\mathbb{C}}D_t^{\gamma}\phi_s(t) = -p_s\phi_s(t) + \sum_{r=1}^{n}\nu_{sr}g_r(\psi_r(t-\varrho_1(t))) + \varphi_s, \\ {}_{0}^{\mathbb{C}}D_t^{\gamma}\psi_s(t) = -q_s\psi_s(t) + w_s\phi_s(t-\varrho_2(t)), \quad s = 1,2,\dots,n, \end{cases} \tag{3} $$

as shown in Fig. 2, where $0 < \gamma < 1$; $\phi_s(t)$ and $\psi_s(t)$ are the of mRNA and protein concentrations of the s^{th} node, respectively; p_s and q_s are positive scalars, which represents the rates of degradation rates of mRNA and protein, respectively; $\mathcal{V} = [\nu_{sr}] \in \mathcal{R}^{q\times q}$ represents the coupling matrix (see [23]); g_r is the form $g_r(\xi) = \frac{\xi^H}{1+\xi^H}$, where H is the Hill coefficient; $\varphi_s = \sum_{r\in I_s}\zeta_{sr}$, I_s is the repressors of gene s; w_s is a constant; $\varrho_1(t)$ and $\varrho_2(t)$ are time-varying delays.

The authors [22] investigated the existence problem of nonnegative equilibrium of FGRNs system (3). We assume that in this section that FGRNs system (3) have at least one nonnegative equilibrium with denoted by (ϕ^*, ψ^*) as follows:

$$ \begin{cases} 0 = -p_s\phi_s^*(\varpi) + \sum_{r=1}^{n}\nu_{sr}g_r(\psi_r^*(\varpi)) + \varphi_s, \\ 0 = -q_s\psi_s^*(\varpi) + w_s\phi_s^*(\varpi), \end{cases} \tag{4} $$

where $\phi^*(\varpi) = \mathrm{col}(\phi_1^*(\varpi), \phi_2^*(\varpi), \dots, \phi_n^*(\varpi))$ and $\psi^*(\varpi) = \mathrm{col}(\psi_1^*(\varpi), \psi_2^*(\varpi), \dots, \psi_n^*(\varpi))$.

Obviously, we define $\alpha_s(t) = \phi_s(t) - \phi_s^*$ and $\beta_s(t) = \psi_s(t) - \psi_s^*$, FGRNs system (3) can be expressed as

$$ \begin{cases} {}_{0}^{\mathbb{C}}D_t^{\gamma}\alpha(t) = -\mathcal{P}\alpha(t) + \mathcal{V}\wp(\beta(t-\varrho_1(t))), \\ {}_{0}^{\mathbb{C}}D_t^{\gamma}\beta(t) = -\mathcal{Q}\beta(t) + \mathcal{W}\alpha(t-\varrho_2(t)), \end{cases} \tag{5} $$

where $\mathcal{P} = \mathrm{diag}(p_1, p_2, \dots, p_m)$, $\mathcal{Q} = \mathrm{diag}(q_1, q_2, \dots, q_m)$, $\mathcal{W} = \mathrm{diag}(w_1, w_2, \dots, w_m)$, $\alpha(t) = \mathrm{col}(\alpha_1(t), \alpha_2(t), \dots, \alpha_m(t))$, $\beta(t) = \mathrm{col}(\beta_1(t), \beta_2(t), \dots, \beta_m(t))$, $\wp(\beta(t)) = \mathrm{col}(\wp_1(\beta_1(t)), \dots, \wp_m(\beta_m(t)))$, $\wp_i(\beta_i(t)) = g_i(\beta_i(t)+\beta^*) - g_i(\beta_i^*)$.

Then control system (5) can be represented as

$$ \begin{cases} {}_{0}^{\mathbb{C}}D_t^{\gamma}\alpha(t) = -\mathcal{P}\alpha(t) + \mathcal{V}\wp(\beta(t-\varrho_1(t))) + u_i(t), \\ {}_{0}^{\mathbb{C}}D_t^{\gamma}\beta(t) = -\mathcal{Q}\beta(t) + \mathcal{W}\alpha(t-\varrho_2(t)) + u_j(t), \end{cases} \tag{6} $$

where $u_i(t)$ and $u_j(t)$ are control inputs.

The initial value of system (6) is given as follows

$$ \begin{cases} \alpha(t) = \theta(t), & t \in [-\varrho, 0], \\ \beta(t) = \hat{\theta}(t), & t \in [-\varrho, 0], \end{cases} \tag{7} $$

where $\varrho = \max\{\varrho_1, \varrho_2\}$. $\theta(t)$ and $\hat{\theta}(t)$ is bounded and continuous function on $[-\varrho, 0]$.

An impulsive controller is designed as

$$ \begin{cases} u_i(t) = \Theta_1\alpha(t)\delta(t-t_{\sigma+1}), & t \in [t_\sigma, t_{\sigma+1}), \quad \sigma \in \mathcal{Z}_+, \\ u_j(t) = \Theta_2\beta(t)\delta(t-t_{\sigma+1}), & t \in [t_\sigma, t_{\sigma+1}), \quad \sigma \in \mathcal{Z}_+, \end{cases} \tag{8} $$

where $\delta(\cdot)$ is the Dirac delta function; $\Theta_1, \Theta_2 \in \mathcal{R}^{m\times m}$ are the gain matrices.

By using impulsive controller (8), the system (6) can be expressed as

$$ \begin{cases} {}_{0}^{\mathbb{C}}D_t^{\gamma}\alpha(t) = -\mathcal{P}\alpha(t) + \mathcal{V}\wp(\beta(t-\varrho_1(t))), & t \in [t_\sigma, t_{\sigma+1}), \\ {}_{0}^{\mathbb{C}}D_t^{\gamma}\beta(t) = -\mathcal{Q}\beta(t) + \mathcal{W}\alpha(t-\varrho_2(t)), & t \in [t_\sigma, t_{\sigma+1}), \\ \Delta\alpha(t) = \Theta_1\alpha(t_\sigma^-), & \sigma \in \mathcal{Z}_+, \\ \Delta\beta(t) = \Theta_2\beta(t_\sigma^-), & \sigma \in \mathcal{Z}_+, \end{cases} \tag{9} $$

where $\Delta\alpha(t) = \alpha(t_\sigma) - \alpha(t_\sigma^-)$, $\alpha(t_\sigma) = \alpha(t_\sigma^+)$ and $\alpha(t_\sigma^-) = \lim_{t\to t_{\sigma^-}}\alpha(t)$; $\Delta\beta = \beta(t_\sigma) - \beta(t_\sigma^-)$, $\beta(t_\sigma) = \beta(t_\sigma^+)$ and $\beta(t_\sigma^-) = \lim_{t\to t_{\sigma^-}}\beta(t)$.

Assumption 1. There exist constants ξ_i^+ and ξ_i^- such that the regulatory function $\hbar_i(\cdot)$ satisfies

$$ \xi_i^- \leq \frac{\hbar_i(a) - \hbar_i(\hat{a})}{a - \hat{a}} \leq \xi_i^+, $$

for all $\hat{a}, a \in \mathcal{R}$ with $a \neq \hat{a}$.

Definition 2.3 ([36]). The FTMLS with initial conditions is the trivial solution of system (9), if there exist positive constants $\{\delta, \epsilon, \gamma, \varrho, T\}$ with $\|\theta(t)\| + \|\hat{\theta}(t)\| \leq \delta$ such that $\|\alpha(t)\| + \|\beta(t)\| \leq (\|\theta(t)\| + \|\hat{\theta}(t)\|)\{\mathbf{E}_\gamma(-\eta t^\gamma)\}^\varrho < \epsilon$, $\forall t \in [0, T]$.

Lemma 2.4 ([23]). *Let $\alpha(t)$ be a vector function that is continuously differentiable on t, then*

$$ {}_{t_0}^{\mathbb{C}}D_t^{\gamma}\alpha^T(t)\alpha(t) \leq 2\alpha^T(t){}_{t_0}^{\mathbb{C}}D_t^{\gamma}\alpha(t), $$

where $0 < \gamma \leq 1$ and $t > t_0$. We denote ${}_{0}^{\mathbb{C}}D_t^{\gamma}\alpha(t)$ Caputo fractional derivative as D^γ.

Lemma 2.5 ([39]). *Let $\hat{\gamma} = (\hat{\gamma}_1, \hat{\gamma}_2, \dots, \hat{\gamma}_q)^T \in \mathcal{R}^q$ and $\hat{\delta} = (\hat{\delta}_1, \hat{\delta}_2, \dots, \hat{\delta}_q)^T \in \mathcal{R}^q$. If $\|\hat{\delta}\| \leq 1$, then $\mathbf{sat}(\hat{\delta}) \in \mathbf{co}\{\mho_s\hat{\delta} + \mho_s^-\hat{\delta},\ s \in \aleph\}$, where $\mho = \{\mho_s \in \aleph\}$ denotes the set of $s \times s$ diagonal matrices with diagonal elements of 0 or 1 and $\mho_s^- = I - \mho_s$.*

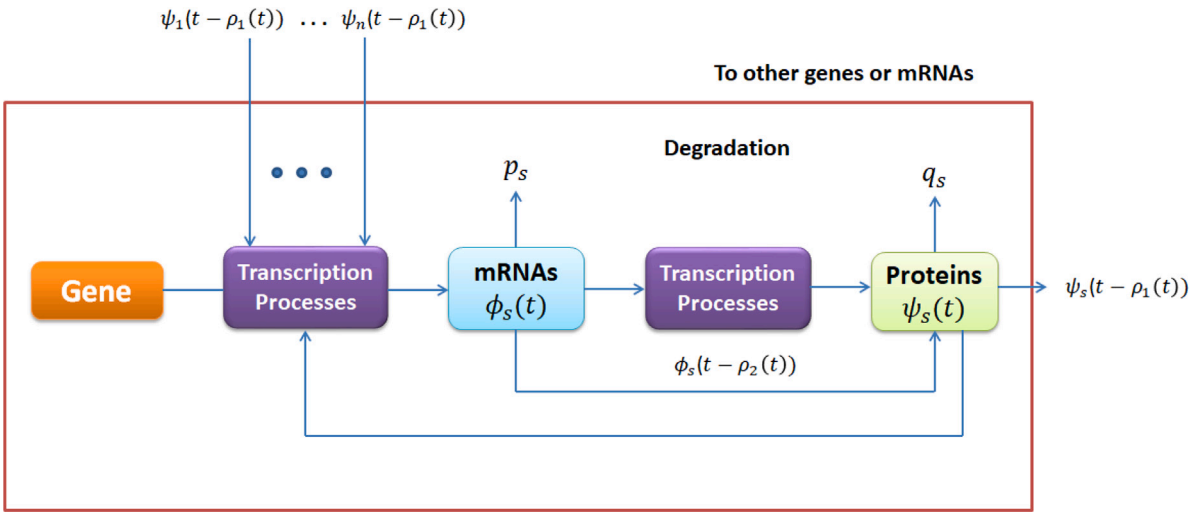

Fig. 2. Flow chart for the GRNs model (3).

3. Main results

In this section, we derive a sufficient condition for the finite-time Mittag-Leffler stabilization problem of fractional-order genetic regulatory networks system (6) via impulsive control with actuator saturation.

We denote that for convenience

$$Y_1 = \operatorname{diag}\left(\xi_1^-\xi_1^+, \xi_2^-\xi_2^+, \dots, \xi_q^-\xi_q^+\right) \text{ and}$$
$$Y_2 = \operatorname{diag}\left(\frac{\xi_1^- + \xi_1^+}{2}, \frac{\xi_2^- + \xi_2^+}{2}, \dots, \frac{\xi_q^- + \xi_q^+}{2}\right).$$

3.1. Stabilization control mechanism for fractional-order genetic regulatory networks via an impulsive control

The finite-time Mittag-Leffler stabilization criteria for fractional-order genetic regulatory networks system (9) with impulsive control are derived based on Lyapunov functional and linear matrix inequalities approach in the following sub-sections.

Theorem 3.1. *For given scalars η_1, η_2, μ_1, μ_2, ϵ, δ, two matrices $\Omega_1 > 0$, $\Omega_2 > 0$, diagonal matrices $Y_1 > 0$, $Y_2 > 0$, symmetric matrices Λ_1, Λ_2, and arbitrary matrices Δ_1, Δ_2 with $\Theta_1 = \Omega_1^{-1}\Delta_1 - I$ and $\Theta_2 = \Omega_2^{-1}\Delta_2 - I$, the system (9) is FTMLS if the following inequalities*

$$(i)\ \begin{pmatrix} -\mu_1\Omega_1 & \Delta_1^T \\ * & -\Omega_1 \end{pmatrix} \le 0 \quad \text{and} \quad \begin{pmatrix} -\mu_2\Omega_2 & \Delta_2^T \\ * & -\Omega_2 \end{pmatrix} \le 0, \tag{10}$$

$$(ii)\ \begin{bmatrix} -(\Omega_1\mathcal{P} + \mathcal{P}^T\Omega_1 - \Lambda_1) & 0 \\ * & -(\Omega_2\mathcal{Q} + \mathcal{Q}^T\Omega_2 - \Lambda_2) \end{bmatrix} < 0, \tag{11}$$

$$(iii)\ \begin{bmatrix} F - \Lambda_1 + \eta_1\Omega_1 & 0 & 0 & \Omega_1\mathcal{V} \\ * & -Y_1F - \Lambda_2 & \Omega_2\mathcal{W} + \eta_2\Omega_2 & Y_2F \\ * & * & F & 0 \\ * & * & * & -F \end{bmatrix} < 0, \tag{12}$$

$$(iv)\ \left(\hat{\wp}\mathbf{E}_\gamma(-\eta t^\gamma)\right)^{\frac{1}{2}} < \frac{\epsilon}{\delta}, \tag{13}$$

where

$$\hat{\wp} = \frac{\mu\lambda_{\max}(\Omega)}{\lambda_{\min}(\Omega)}, \lambda_{\min}(\Omega) = \min\{\lambda_{\min}(\Omega_1), \lambda_{\min}(\Omega_2)\}, \text{ and}$$
$$\lambda_{\max}(\Omega) = \max\{\lambda_{\max}(\Omega_1), \lambda_{\max}(\Omega_2)\}.$$

Proof. Take the Lyapunov function as

$$\mathbf{V}(t) = \alpha^T(t)\Omega_1\alpha(t) + \beta^T(t)\Omega_2\beta(t). \tag{14}$$

It follow from the Eq. (10), it can see that

$$\begin{pmatrix} -\mu_1\Omega_1 & \Delta_1^T \\ * & -\Omega_1 \end{pmatrix} \le 0$$
$$\Leftrightarrow \begin{pmatrix} I & (I+\Theta_1)^T \\ 0 & I \end{pmatrix}\begin{pmatrix} -\mu_1\Omega_1 & \Delta_1^T \\ * & -\Omega_1 \end{pmatrix}\begin{pmatrix} I & 0 \\ I+\Theta_1 & I \end{pmatrix} \le 0$$
$$\Leftrightarrow \begin{pmatrix} -\mu_1\Omega_1 + (I+\Theta_1)^T\Omega_1(I+\Theta_1) & 0 \\ * & -\Omega_1 \end{pmatrix} \le 0$$
$$\Leftrightarrow -\mu_1\Omega_1 + (I+\Theta_1)^T\Omega_1(I+\Theta_1) \le 0,$$

and

$$\begin{pmatrix} -\mu_2\Omega_2 & \Delta_2^T \\ * & -\Omega_2 \end{pmatrix} \le 0$$
$$\Leftrightarrow \begin{pmatrix} I & (I+\Theta_2)^T \\ 0 & I \end{pmatrix}\begin{pmatrix} -\mu_2\Omega_2 & \Delta_2^T \\ * & -\Omega_2 \end{pmatrix}\begin{pmatrix} I & 0 \\ I+\Theta_2 & I \end{pmatrix} \le 0$$
$$\Leftrightarrow \begin{pmatrix} -\mu_2\Omega_2 + (I+\Theta_2)^T\Omega_2(I+\Theta_2) & 0 \\ * & -\Omega_2 \end{pmatrix} \le 0$$
$$\Leftrightarrow -\mu_2\Omega_2 + (I+\Theta_2)^T\Omega_2(I+\Theta_2) \le 0,$$

when $t = t_\sigma$, we obtain that

$$\begin{aligned}\mathbf{V}(t_\sigma) =& \alpha^T(t_\sigma)\Omega_1\alpha(t_\sigma) + \beta^T(t_\sigma)\Omega_2\beta(t_\sigma)\\ \le& \alpha^T(t_\sigma^-)(I+\Theta_1)^T\Omega_1(I+\Theta_1)\alpha(t_\sigma^-)\\ &+ \beta^T(t_\sigma^-)(I+\Theta_2)^T\Omega_2(I+\Theta_2)\beta(t_\sigma^-)\\ \le& \mu_1\alpha^T(t_\sigma^-)\Omega_1\alpha(t_\sigma^-) + \mu_2\beta^T(t_\sigma^-)\Omega_2\beta(t_\sigma^-)\\ \le& \mu\mathbf{V}(t_\sigma^-),\end{aligned} \tag{15}$$

where $\mu = \max\{\mu_1, \mu_2\}$.

For $t \in [t_\sigma, t_{\sigma+1})$, by using Lemma 2.4 and computing the derivatives of $V(t)$, obtain that

$$\begin{aligned}D^\gamma\mathbf{V}(t) \le& 2\alpha^T(t)\Omega_1D^\gamma\alpha(t) + 2\beta^T(t)\Omega_2D^\gamma\beta(t)\\ \le& 2\alpha^T(t)\Omega_1\left(-\mathcal{P}\alpha(t) + \mathcal{V}\hbar(\beta(t-\rho_1(t)))\right)\\ &+ 2\beta^T(t)\Omega_2\left(-\mathcal{Q}\beta(t) + \mathcal{W}\alpha(t-\rho_2(t))\right)\\ \le& \alpha^T(t)\left(-(\Omega_1\mathcal{P} + \mathcal{P}^T\Omega_1)\right)\alpha(t) + 2\alpha^T(t)\Omega_1\hbar(\beta(t-\rho_1(t)))\\ &+ \beta^T(t)\left(-(\Omega_2\mathcal{Q} + \mathcal{Q}^T\Omega_2)\right)\beta(t) + 2\beta^T(t)\Omega_2\mathcal{W}\alpha(t-\rho_2(t))\\ \le& -\alpha^T(t)(\Omega_1\mathcal{P} + \mathcal{P}^T\Omega_1)\alpha(t) + 2\alpha^T(t)\Omega_1\hbar(\beta(t-\rho_1(t)))\\ &- \beta^T(t)(\Omega_2\mathcal{Q} + \mathcal{Q}^T\Omega_2)\beta(t) + 2\beta^T(t)\Omega_2\mathcal{W}\alpha(t-\rho_2(t))\\ \le& \begin{bmatrix} \alpha(t) & \beta(t) \end{bmatrix}\begin{bmatrix} -(\Omega_1\mathcal{P} + \mathcal{P}^T\Omega_1) & 0 \\ * & -(\Omega_2\mathcal{Q} + \mathcal{Q}^T\Omega_2) \end{bmatrix}\begin{bmatrix} \alpha(t) \\ \beta(t) \end{bmatrix}\\ &+ 2\alpha^T(t)\Omega_1\mathcal{V}\hbar(\beta(t-\rho_1(t))) + 2\beta^T(t)\Omega_2\mathcal{W}\alpha(t-\rho_2(t)).\end{aligned} \tag{16}$$

Its observe that

$$(\hbar_i(\beta_i(t-\varrho_1(t)))-\xi_i^-\beta_i(t))(\hbar_i(\beta_i(t-\varrho_1(t)))-\xi_i^+\beta_i(t))\le 0,$$
$$-\big(\alpha^T(t)\alpha(t)+\alpha^T(t-\varrho_2(t))\alpha(t-\varrho_2(t))\big)\le 0,$$

for every $i\in\wedge$, and is equivalent to

$$\begin{bmatrix} \alpha(t) & \beta(t) & \alpha(t-\varrho_2(t)) & \hbar(\beta(t-\varrho_1(t))) \end{bmatrix} \times \begin{bmatrix} -e_ie_i^T & 0 & 0 & 0 \\ * & \xi_i^-\xi_i^+e_ie_i^T & 0 & -\frac{\xi_i^-+\xi_i^+}{2}e_ie_i^+ \\ * & * & -e_ie_i^T & 0 \\ * & * & * & e_ie_i^T \end{bmatrix} \times \begin{bmatrix} \alpha(t) \\ \beta(t) \\ \alpha(t-\varrho_2(t)) \\ \hbar(\beta(t-\varrho_1(t))) \end{bmatrix} \le 0,$$

for each $i\in\wedge$, where $\hat{\varepsilon}_i$ represents the unit column vector, which one element on its ith row and zeros elsewhere.

Then

$$\sum_{i=1}^{m} f_i \begin{bmatrix} \alpha(t) & \beta(t) & \alpha(t-\varrho_2(t)) & \hbar(\beta(t-\varrho_1(t))) \end{bmatrix} \times \begin{bmatrix} -\hat{\varepsilon}_i\hat{\varepsilon}_i^T & 0 & 0 & 0 \\ * & \xi_i^-\xi_i^+\hat{\varepsilon}_i\hat{\varepsilon}_i^T & 0 & -\frac{\alpha_i^-+\xi_i^+}{2}\hat{\varepsilon}_i\hat{\varepsilon}_i^+ \\ * & * & -\hat{\varepsilon}_i\hat{\varepsilon}_i^T & 0 \\ * & * & * & \hat{\varepsilon}_i\hat{\varepsilon}_i^T \end{bmatrix} \times \begin{bmatrix} \alpha(t) \\ \beta(t) \\ \alpha(t-\varrho_2(t)) \\ \hbar(\beta(t-\varrho_1(t))) \end{bmatrix} \le 0,$$

which is equivalent to

$$\begin{bmatrix} \alpha(t) & \beta(t) & \alpha(t-\varrho_2(t)) & \hbar(\beta(t-\varrho_1(t))) \end{bmatrix} \begin{bmatrix} F & 0 & 0 & 0 \\ * & -Y_{1F} & 0 & Y_{2F} \\ * & * & F & 0 \\ * & * & * & -F \end{bmatrix} \times \begin{bmatrix} \alpha(t) \\ \beta(t) \\ \alpha(t-\varrho_2(t)) \\ \hbar(\beta(t-\varrho_1(t))) \end{bmatrix} \ge 0, \tag{17}$$

where $F=\mathrm{diag}(f_1,f_2,\dots,f_m)>0$. From Eqs. (16) and (17), we obtain that

$$\begin{aligned} &D^\gamma\mathbf{V}(t) \\ &\le 2\alpha^T(t)\Omega_1\mathcal{V}\hbar(\beta(t-\varrho_1(t)))+2\beta^T(t)\Omega_2\mathcal{W}\alpha(t-\varrho_2(t))+\begin{bmatrix}\alpha(t) & \beta(t)\end{bmatrix} \\ &\times\begin{bmatrix} -(\Omega_1\mathcal{P}+\mathcal{P}^T\Omega_1) & 0 \\ * & -(\Omega_2\mathcal{Q}+\mathcal{Q}^T\Omega_2)\end{bmatrix}\begin{bmatrix}\alpha(t)\\ \beta(t)\end{bmatrix} \\ &+\begin{bmatrix}\alpha(t) & \beta(t) & \alpha(t-\varrho_2(t)) & \hbar(\beta(t-\varrho_1(t)))\end{bmatrix} \\ &\times\begin{bmatrix} F & 0 & 0 & 0 \\ * & -Y_{1F} & 0 & Y_{2F} \\ * & * & F & 0 \\ * & * & * & -F\end{bmatrix}\begin{bmatrix}\alpha(t)\\ \beta(t)\\ \alpha(t-\varrho_2(t))\\ \hbar(\beta(t-\varrho_1(t)))\end{bmatrix} \\ &\le\begin{bmatrix}\alpha(t) & \beta(t)\end{bmatrix}\begin{bmatrix} -(\Omega_1\mathcal{P}+\mathcal{P}^T\Omega_1-\Lambda_1) & 0 \\ * & -(\Omega_2\mathcal{Q}+\mathcal{Q}^T\Omega_2-\Lambda_2)\end{bmatrix} \\ &\times\begin{bmatrix}\alpha(t)\\ \beta(t)\end{bmatrix}+\begin{bmatrix}\alpha(t) & \beta(t)\end{bmatrix} \\ &\times\begin{bmatrix}\eta_1\Omega_1 & 0\\ * & \eta_2\Omega_1\end{bmatrix}\begin{bmatrix}\alpha(t)\\ \beta(t)\end{bmatrix}+\begin{bmatrix}\alpha(t) & \beta(t) & \alpha(t-\varrho_2(t)) & \hbar(\beta(t-\varrho_1(t)))\end{bmatrix} \\ &\times\begin{bmatrix} F-\Lambda_1+\eta_1\Omega_1 & 0 & 0 & \Omega_1\mathcal{V} \\ * & -Y_{1F}-\Lambda_2+\eta_2\Omega_2 & \Omega_2\mathcal{W} & Y_{2F} \\ * & * & F & 0 \\ * & * & * & -F\end{bmatrix}\begin{bmatrix}\alpha(t)\\ \beta(t)\\ \alpha(t-\varrho_2(t))\\ \hbar(\beta(t-\varrho_1(t)))\end{bmatrix} \end{aligned}$$

It follow form the Eqs. (11) and (12), one has

$$\begin{aligned} D^\gamma\mathbf{V}(t) &\le \begin{bmatrix}\alpha(t) & \beta(t)\end{bmatrix}\begin{bmatrix}-\eta_1\Omega_1 & 0\\ * & -\eta_2\Omega_2\end{bmatrix}\begin{bmatrix}\alpha(t)\\ \beta(t)\end{bmatrix} \\ &\le -\eta\mathbf{V}(t), \end{aligned} \tag{18}$$

where $\eta=\min\{\eta_1,\eta_2\}$.

According to Lemma 2 in [23] and Eq. (18), we get

$$\lambda_{\min}(\Omega)\big(\|\alpha(t)\|^2+\|\beta(t)\|^2\big)\le\mathbf{V}(t)\le\mu\mathbb{E}_\gamma(-\eta t^\gamma)V(0),$$

which implies that

$$\lambda_{\min}(\Omega)\big(\|\alpha(t)\|^2+\|\beta(t)\|^2\big)\le\mu\lambda_{\max}(\Omega)\mathbb{E}_\gamma(-\eta t^\gamma)\big(\|\theta(0)\|^2+\|\hat{\theta}(0)\|^2\big).$$

Then

$$\|\alpha(t)\|^2+\|\beta(t)\|^2\le\hat{\wp}\mathbb{E}_\gamma(-\eta t^\gamma)\big(\|\theta(0)\|^2+\|\hat{\theta}(0)\|^2\big).$$

It follow form the Eq. (13) and Definition 2.3, we obtain that $\|\alpha(t)\|+\|\beta(t)\|<\epsilon$. Therefore, the system (9) can be achieved the FTMLS under impulsive control.

Remark 3.2. When the system (9) is simplified to integer-order GRNs with impulsive control as follows:

$$\begin{cases} \dot{\alpha}(t)=-\mathcal{P}\alpha(t)+\mathcal{V}\wp(\beta(t-\varrho_1(t))), & t\in[t_\sigma,t_{\sigma+1}), \\ \dot{\beta}(t)=-\mathcal{Q}\beta(t)+\mathcal{W}\alpha(t-\varrho_2(t)), & t\in[t_\sigma,t_{\sigma+1}), \\ \Delta\alpha(t)=\Theta_1\alpha(t_\sigma^-), & \sigma\in\mathcal{Z}_+, \\ \Delta\beta(t)=\Theta_2\beta(t_\sigma^-), & \sigma\in\mathcal{Z}_+, \end{cases} \tag{19}$$

where $\dot{\alpha}(t)=\frac{d\alpha}{dt}$ and $\dot{\beta}(t)=\frac{d\beta}{dt}$. It follows from Lemma 2 in [23], that the system (9) is Mittag-Leffler stabilization. Therefore, the Mittag-Leffler stabilization criterion of system (9) is expressed into an exponential stabilization of system (19).

Remark 3.3. The stability analysis of FGRNs has been examined previously using the algebraic criteria and the Lyapunov approach [19–23]. In Theorem 3.1, sufficient conditions for FGRNs are given by constructing Lyapunov functions and using the LMI conditions to guarantee FTMLS criteria. We can see from the proof that these stability conditions are formulated algebraic criteria, which may result in less conservative results. The obtained LMI stability criteria have a simpler form than the algebraic stability criteria proposed in (see [19–23]), which reduces computational complexity. Thus, our results have replenished some former works, which implies that our results are new.

Remark 3.4. In the existing works, some results an impulsive control based on the molecular models of neural networks, complex-valued neural networks via actuator saturation [39,40]. Some few authors [41,42], an actuator saturation is a common phenomenon in biological models are studied. Therefore, inspired by [39–42] to study, an impulsive control based on FTMLS problem of FGRNs via actuator saturation.

3.2. Stabilization control mechanism for fractional-order genetic regulatory networks via an impulsive control with actuator saturation

In this sub-section, by applying the polytopic approach and a novel Lyapunov functional, some linear matrix inequalities based sufficient conditions are derived to ensure the finite-time Mittag-Leffler stabilization for the fractional-order genetic regulatory networks with impulsive control and actuator saturation.

We designed the impulsive control with actuator saturation scheme as follows:

$$\begin{cases} u_i(t)=\Xi_1\mathrm{sat}(\hbar_1(t))\delta(t-t_\sigma), & \sigma\in\mathbb{Z}_+, \\ u_j(t)=\Xi_2\mathrm{sat}(\hbar_2(t))\delta(t-t_\sigma), & \sigma\in\mathbb{Z}_+, \end{cases} \tag{20}$$

where Ξ_1 and Ξ_2 are constant matrices; $\hbar_1(t) = \Psi_1\alpha(t)$ and $\hbar_2(t) = \Psi_2\beta(t)$ with $\Psi_1 \in \mathcal{R}^{q\times q}$, $\Psi_2 \in \mathcal{R}^{q\times q}$ is the control gain matrices.

Considering controllers (20), the dynamical system (6) is rewritten as

$$\begin{cases} D^{\gamma}\alpha(t) = -\mathcal{P}\alpha(t) + \mathcal{V}\wp(\beta(t-\varrho_1(t))), \quad t\in[t_\sigma, t_{\sigma+1}),\\ D^{\gamma}\beta(t) = -\mathcal{Q}\beta(t) + \mathcal{W}\alpha(t-\varrho_2(t)), \quad t\in[t_\sigma, t_{\sigma+1}),\\ \Delta\alpha(t_\sigma) = \Xi_1\mathrm{sat}(\Psi_1\alpha(t_\sigma^-)), \quad \sigma\in\mathcal{Z}_+,\\ \Delta\beta(t_\sigma) = \Xi_2\mathrm{sat}(\Psi_2\beta(t_\sigma^-)), \quad \sigma\in\mathcal{Z}_+, \end{cases} \tag{21}$$

Furthermore, based on Lemma 2.5 in system (21), for two matrices $\Psi_1 \in \mathcal{R}^{q\times q}$ and $\mathcal{H}\in\mathcal{R}^{q\times q}$. If $\|\mathcal{H}\alpha(t)\|_\infty \le 1$, then

$$\mathrm{sat}(\Psi_1\alpha(t)) \in \mathrm{co}\{\mathfrak{V}_\ell\Psi_1\alpha(t) + \mathfrak{V}_\ell^{-1}\mathcal{H}\alpha(t),\ \ell\in\aleph\}.$$

For $\Psi_2\in\mathcal{R}^{q\times q}$ and $\mathcal{L}\in\mathcal{R}^{q\times q}$. If $\|\mathcal{L}\beta(t)\|_\infty \le 1$, then

$$\mathrm{sat}(\Psi_2\beta(t)) \in \mathrm{co}\{\mathfrak{V}_\ell\Psi_2\beta(t) + \mathfrak{V}_\ell^{-1}\mathcal{L}\beta(t),\ \ell\in\aleph\}.$$

Furthermore

$$\begin{cases} \forall\ \alpha(t)\in\mathcal{E}\big(|\mathcal{H}|,1\big) = \{\alpha(t)\in\mathcal{R}^q; \|\mathcal{H}\alpha(t)\|_\infty \le 1\},\\ \forall\ \beta(t)\in\mathcal{E}\big(|\mathcal{L}|,1\big) = \{\beta(t)\in\mathcal{R}^q; \|\mathcal{L}\beta(t)\|_\infty \le 1\}. \end{cases}$$

It can see that

$$\begin{cases} \mathrm{sat}(\Psi_1\alpha(t)) \in \mathrm{co}\{\mathfrak{V}_\ell\Psi_1\alpha(t) + \mathfrak{V}_\ell^{-1}\mathcal{H}\alpha(t),\ \ell\in\aleph\},\\ \mathrm{sat}(\Psi_2\beta(t)) \in \mathrm{co}\{\mathfrak{V}_\ell\Psi_2\beta(t) + \mathfrak{V}_\ell^{-1}\mathcal{L}\beta(t),\ \ell\in\aleph\}, \end{cases}$$

that is

$$\mathrm{sat}(\Psi_1\alpha(t)) = \sum_{\ell=1}^{2^q}\lambda_\ell(\alpha(t))\big(\mathfrak{V}_\ell\Psi_1 + \mathfrak{V}_\ell^{-1}\mathcal{H}\big)\alpha(t), \tag{22}$$

with $\sum_{\ell=1}^{2^q}\lambda_\ell(\alpha(t)) = 1$, $0\le\lambda_\ell(\alpha(t))\le 1$.

Similarly

$$\mathrm{sat}(\Psi_2\beta(t)) = \sum_{\ell=1}^{2^q}\lambda_\ell(\beta(t))\big(\mathfrak{V}_\ell\Psi_2 + \mathfrak{V}_\ell^{-1}\mathcal{L}\big)\beta(t) \tag{23}$$

with $\sum_{\ell=1}^{2^q}\lambda_\ell(\beta(t)) = 1$, $0\le\lambda_\ell(\beta(t))\le 1$.

Based on Eq. (22) and Eq. (23), the result of Eq. (21) is

$$\begin{cases} D^{\gamma}\alpha(t) = -\mathcal{P}\alpha(t) + \mathcal{V}\wp(\beta(t-\varrho_1(t))) \quad t\in[t_\sigma, t_{\sigma+1}),\\ D^{\gamma}\beta(t) = -\mathcal{Q}\beta(t) + \mathcal{W}\alpha(t-\varrho_2(t)), \quad t\in[t_\sigma, t_{\sigma+1}),\\ \Delta\alpha(t_\sigma) = \big[I_q + \Xi_1\sum_{\ell=1}^{2^q}\lambda_\ell(\alpha(t_\sigma))\big(\mathfrak{V}_\ell\Psi_1 + \mathfrak{V}_\ell^{-1}\mathcal{H}\big)\big]\alpha(t_\sigma^-),\ \sigma\in\mathcal{Z}_+,\\ \Delta\beta(t_\sigma) = \big[I_q + \Xi_2\sum_{\ell=1}^{2^q}\lambda_\ell(\beta(t_\sigma))\big(\mathfrak{V}_\ell\Psi_2 + \mathfrak{V}_\ell^{-1}\mathcal{L}\big)\big]\beta(t_\sigma^-),\ \sigma\in\mathcal{Z}_+. \end{cases} \tag{24}$$

Remark 3.5. The actuator saturation term in the nonlinear dynamical FGRNs system (24) by applying the polytopic approach of Lemma 2.5 in this article. In future study, we will be able to discuss the stabilization problem of the proposed model using the sector nonlinearity model technique to deal with the actuator saturation term given in [41,42].

Theorem 3.6. *For given scalars η_1, η_2, $\hat{\mu}_1$, $\hat{\mu}_2$, ϵ, δ, two matrices $\Omega_1 > 0$, $\Omega_2 > 0$, diagonal matrices $Y_1 > 0$, $Y_2 > 0$, symmetric matrices Λ_1, Λ_2 and arbitrary matrices Δ_1, Δ_2, the system (24) is FTMLS if the following inequalities*

$$(i)\ \begin{bmatrix} -\hat{\mu}_1\Omega_1 & \big(I_q + \Xi_1\big(\mathfrak{V}_\ell\Psi_1 + \mathfrak{V}_\ell^{-1}\mathcal{H}\big)\big)^T\\ * & -\Omega_1 \end{bmatrix} \le 0, \tag{25}$$

$$(ii)\ \begin{bmatrix} -\hat{\mu}_2\Omega_2 & \big(I_q + \Xi_2\big(\mathfrak{V}_\ell\Psi_2 + \mathfrak{V}_\ell^{-1}\mathcal{L}\big)\big)^T\\ * & -\Omega_2 \end{bmatrix} \le 0, \tag{26}$$

$$(iii)\ \begin{bmatrix} -(\Omega_1\mathcal{P} + \mathcal{P}^T\Omega_1 - \Lambda_1) & 0\\ * & -(\Omega_2\mathcal{Q} + \mathcal{Q}^T\Omega_2 - \Lambda_2) \end{bmatrix} < 0, \tag{27}$$

$$(iv)\ \begin{bmatrix} F - \Lambda_1 + \eta_1\Omega_1 & 0 & 0 & \Omega_1\mathcal{V}\\ * & -Y_1F - \Lambda_2 & \Omega_2\mathcal{W} + \eta_2\Omega_2 & Y_2F\\ * & * & F & 0\\ * & * & * & -F \end{bmatrix} < 0, \tag{28}$$

$$(v)\ \big(\breve{\wp}_\kappa\mathbf{E}_\gamma(-\eta t^\gamma)\big)^{\frac{1}{2}} < \frac{\epsilon}{\delta}, \tag{29}$$

where $\breve{\wp}_\kappa = \frac{\breve{\mu}\lambda_{\max}(\Omega)}{\lambda_{\min}(\Omega)}$.

Proof. Choose Lyapunov function

$$\mathbf{V}(t) = \alpha^T(t)\Omega_1\alpha(t) + \beta^T(t)\Omega_2\beta(t). \tag{30}$$

By computing the derivative of the Lyapunov function $\mathbf{V}(t)$ along the solution of the system (24), then by applying Lemma 2.4 one has

$$D^{\gamma}\mathbf{V}(t) \le 2\alpha^T(t)\Omega_1 D^{\gamma}\alpha(t) + 2\beta^T(t)\Omega_2 D^{\gamma}\beta(t)$$

The remaining proof is the same as Eqs. (16)–(18) in Theorem 3.1, for $t\in[t_\sigma, t_{\sigma+1})$

$$D^{\gamma}\mathbf{V}(t) \le -\eta\mathbf{V}(t), \tag{31}$$

where $\eta = \min\{\eta_1, \eta_2\}$.

It follow from the Eqs. (25) and (26), it can see that

$$\begin{bmatrix} -\hat{\mu}_1\Omega_1 & \big(I_q + \Xi_1\big(\mathfrak{V}_\ell\Psi_1 + \mathfrak{V}_\ell^{-1}\mathcal{H}\big)\big)^T\\ * & -\Omega_1 \end{bmatrix} \le 0$$
$$\Leftrightarrow \big(I_q + \Xi_1(\mathfrak{V}_\ell\Psi_1 + \mathfrak{V}_\ell^{-}\mathcal{H})\big)^T\Omega_1\big(I_q + \Xi_1(\mathfrak{V}_\ell\Psi_2 + \mathfrak{V}_\ell^{-}\mathcal{H})\big) - \hat{\mu}_1\Omega_1 \le 0,$$

and

$$\begin{bmatrix} -\hat{\mu}_2\Omega_2 & \big(I_q + \Xi_2\big(\mathfrak{V}_\ell\Psi_2 + \mathfrak{V}_\ell^{-1}\mathcal{L}\big)\big)^T\\ * & -\Omega_2 \end{bmatrix} \le 0$$
$$\Leftrightarrow \big(I_q + \Xi_2(\mathfrak{V}_\ell\Psi_2 + \mathfrak{V}_\ell^{-}\mathcal{L})\big)^T\Omega_2\big(I_q + \Xi_2(\mathfrak{V}_\ell\Psi_2 + \mathfrak{V}_\ell^{-}\mathcal{L})\big) - \hat{\mu}_2\Omega_2 \le 0.$$

When $t = t_\sigma$ in Eq. (30), it can see that

$$\begin{aligned} V(\alpha(t_\sigma),\beta(t_\sigma)) =& \alpha^T(t_\sigma^-)\big(I_q + \Xi_1(\mathfrak{V}_\ell\Psi_1 + \mathfrak{V}_\ell^{-}\mathcal{H})\big)^T\Omega_1\\ &\times\big(I_q + \Xi_1(\mathfrak{V}_\ell\Psi_1 + \mathfrak{V}_\ell^{-}\mathcal{H})\big)\alpha(t_\sigma^-)\\ &+ \beta^T(t_\sigma^-)\big(I_q + \Xi_2(\mathfrak{V}_\ell\Psi_2 + \mathfrak{V}_\ell^{-}\mathcal{L})\big)^T\Omega_2\\ &\times\big(I_q + \Xi_2(\mathfrak{V}_\ell\Psi_2 + \mathfrak{V}_\ell^{-}\mathcal{L})\big)\beta(t_\sigma^-)\\ \le&\hat{\mu}_1\alpha^T(t_\sigma^-)\Omega_1\alpha(t_\sigma^-) + \hat{\mu}_2\beta^T(t_\sigma^-)\Omega_2\beta(t_\sigma^-)\\ \le&\breve{\mu}V(\alpha(t),\beta(t)), \end{aligned} \tag{32}$$

where $\breve{\mu} = \min\{\hat{\mu}_1, \hat{\mu}_2\}$. From Eqs. (31) and (32) with by using Lemma 2 in [23], we get

$$\lambda_{\min}(\Omega)\big(\|\alpha(t)\|^2 + \|\beta(t)\|^2\big) \le \breve{\mu}\lambda_{\max}(\Omega)\mathbb{E}_\gamma(-\eta t^\gamma)\big(\|\theta(0)\|^2 + \|\hat{\theta}(0)\|^2\big).$$

Then

$$\|\alpha(t)\|^2 + \|\beta(t)\|^2 \le \breve{\wp}\mathbb{E}_\gamma(-\eta t^\gamma)\big(\|\theta(0)\|^2 + \|\hat{\theta}(0)\|^2\big).$$

It follow form the Eq. (29) and Definition 2.3, we obtain that $\|\alpha(t)\| + \|\beta(t)\| < \epsilon$. Therefore, the system (24) can be achieved the FTMLS via impulsive actuator saturation.

Remark 3.7. When the system (24) is simplified to integer-order GRNs via impulsive control with actuator saturation as follows:

$$\begin{cases} \dot{\alpha}(t) = -\mathcal{P}\alpha(t) + \mathcal{V}\wp(\beta(t-\varrho_1(t))), \quad t\in[t_\sigma, t_{\sigma+1}),\\ \dot{\beta}(t) = -\mathcal{Q}\beta(t) + \mathcal{W}\alpha(t-\varrho_2(t)), \quad t\in[t_\sigma, t_{\sigma+1}),\\ \Delta\alpha(t_\sigma) = \big[I_q + \Xi_1\sum_{\ell=1}^{2^q}\lambda_\ell(\alpha(t_\sigma))\big(\mathfrak{V}_\ell\Psi_1 + \mathfrak{V}_\ell^{-1}\mathcal{H}\big)\big]\alpha(t_\sigma^-),\ \sigma\in\mathcal{Z}_+,\\ \Delta\beta(t_\sigma) = \big[I_q + \Xi_2\sum_{\ell=1}^{2^q}\lambda_\ell(\beta(t_\sigma))\big(\mathfrak{V}_\ell\Psi_2 + \mathfrak{V}_\ell^{-1}\mathcal{L}\big)\big]\beta(t_\sigma^-),\ \sigma\in\mathcal{Z}_+, \end{cases} \tag{33}$$

where $\dot{\alpha}(t) = \frac{d\alpha}{dt}$, and $\dot{\beta}(t) = \frac{d\beta}{dt}$. It follows from Lemma 2 in [23], that the system (24) is Mittag-Leffler stabilization. Therefore, the Mittag-Leffler stabilization criterion of system (24) is expressed into an exponential stabilization of system (33).

Remark 3.8. Compared with the previous studies (see [19–23]), the following are the key aspects and benefits of this article: (i) More

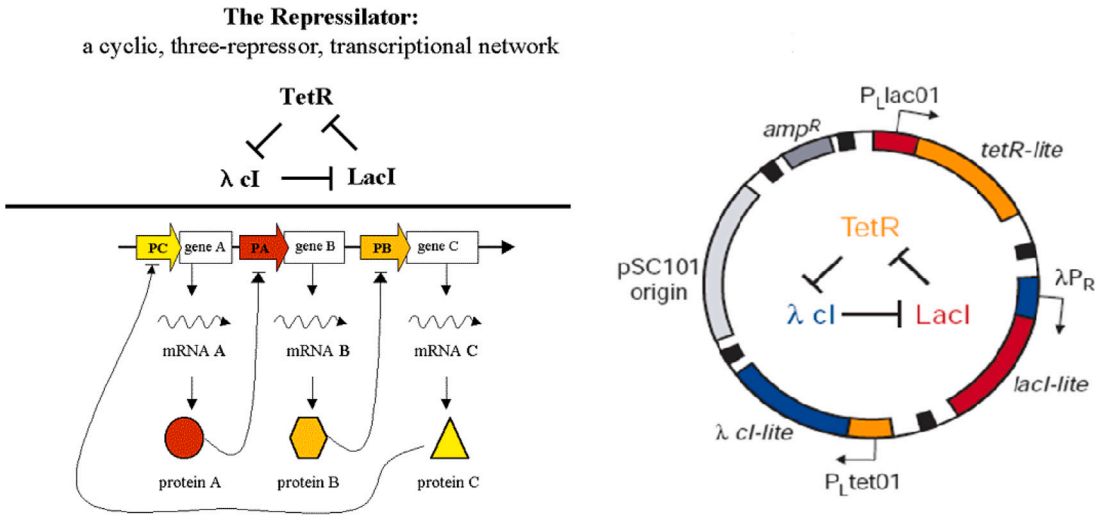

Fig. 3. The repressilator model in [12].

information about FGRNs is used in the LMIs approaches used in this article. (ii) Some effective control gain matrices are designed. (iii) The saturation nonlinearity are handled by polytopic representation approaches. This results in less conservative FTMLS criteria.

Remark 3.9. The authors [23] studied an impulsive control strategy as well as Mittag-Leffler stability for FGRNs utilizing the fractional Lyapunov technique. Unlike existing works [23], we consider actuator saturation in the design of the impulsive controller. Based on the established LMIs, we provide the relatively least conservative conditions to ensure the FTMLS of nonlinear dynamic FGRNs.

Remark 3.10. Using impulsive fractional differential inequality and Lyapunov functions, the author [23] investigated the Mittag-Leffler stability of FGRNs under impulsive control. These classic approaches cannot be directly used to examine FTMLS of FGRNs with impulsive control and actuator saturation. In this article, we investigate the FTMLS of the considered model by combining the advantages of polytopic representation approaches.

4. Numerical examples

In this section, two examples are discussed to illustrate the main theoretical results proposed in this article. The Example 4.1 is concerned with a synthetic oscillatory network of transcriptional regulators with three repressor-protein concentrations and their corresponding mRNA concentrations. Example 4.2 considers a class of fractional-order genetic regulatory networks system (6) under impulsive control with actuator saturation.

Example 4.1. We consider a repressilator model [11,22] to verify that the derived LMI conditions can be used to design the controller for FGRNs. The repressilator is a cyclic negative-feedback loop consisting of three repressor genes (*lacI*, *tetR* and *cI*) and their promoters. Fig. 3 shows the repressilator, which is divided into three genes. Consider the following six connected fractional-order differential models of kinetics systems:

$$\begin{cases} {}_0^{\mathbb{C}}D_t^{\gamma}\alpha_s(t) = \hat{\xi}_s\alpha_s(t) + \frac{\chi_s}{1+\beta_r^H(t-\varrho_1(t))} + \chi_0, \\ {}_0^{\mathbb{C}}D_t^{\gamma}\beta_s(t) = -\phi_s\beta_s(t) - \hat{\omega}_s\alpha_s(t-\varrho_2(t)), \\ s = lacI, tet\ R, cI; r = cI, lacI, tet\ R, \end{cases} \tag{34}$$

where are the α_s and β_s concentrations of the three mRNA and repressor-protein; $\hat{\xi}_s > 0$ and $\phi_s > 0$ represents the mRNA and protein degradation rates, respectively; $\hat{\omega}_s$ represents the sth translation rate from mRNA to protein.

The SUM logic proposed in [11], one has

$$\frac{\chi_s}{1+\beta_r^H(t-\varrho_1(t))} = -\chi_s\Big(1 - \frac{\beta_r^H(t-\varrho_1(t))}{1+\beta_r^H(t-\varrho_1(t))}\Big).$$

It is clear from the FGRNs model (34) that

$$\begin{cases} {}_0^{\mathbb{C}}D_t^{\gamma}\alpha_s(t) = \hat{\xi}_s\alpha_s(t) + \frac{\chi_s\beta_r^H(t-\varrho_1(t))}{1+\beta_r^H(t-\varrho_1(t))} - \chi_s + \chi_0, \\ {}_0^{\mathbb{C}}D_t^{\gamma}\beta_s(t) = -\phi_s\beta_s(t) - \hat{\omega}_s\alpha_s(t-\varrho_2(t)). \end{cases} \tag{35}$$

The parameters are select as follows $\gamma = 0.97$, $\hat{\xi}_s = 2$, $\chi_s = 2.5$, $\phi_s = 1$, $\hat{\omega}_s = 0.9$, $\chi_0 = 0$, $(s = 1, 2, 3)$, $\varrho_1(t) = 2.3|\cos(t)|$, $\varrho_2(t) = 1.5|\sin(t)|$, $G_1 = 0$, $G_2 = 0$, $G_3 = \mathrm{diag}(1, 1, 1)$ and the system matrices can be obtained as $\mathcal{P} = \mathrm{diag}(0.4780, 0.4780, 0.4780)$, $\mathcal{W} = \mathrm{diag}(0.4780, 0.4780, 0.4780)$, $\mathcal{Q} = \mathrm{diag}(0.6432, 0.4046, 0.6432)$ and $\mathcal{V} = \begin{bmatrix} 0 & 0 & -0.2375 \\ -0.2375 & 0 & 0 \\ 0 & -0.2375 & 0 \end{bmatrix}$. The initial values of concentrations of the mRNAs and proteins of system (35) are set as $\phi(0) = [3, 1, 3]^T$ and $\psi(0) = [2, 5, 1]^T$, respectively. Fig. 4 give the phase graph for unstable positions of systems (35). Fig. 5 shows the trajectories of the mRNA and protein concentration states $\alpha_s(t)$ and $\beta_s(t)$ $(s = 1, 2, 3)$, revealing that the system (35) without control input is unstable.

Therefore, the controlled system can be obtained as follows:

$$\begin{cases} {}_0^{\mathbb{C}}D_t^{\gamma}\alpha_s(t) = \hat{\xi}_s\alpha_s(t) + \frac{\chi_s\beta_r^H(t-\varrho_1(t))}{1+\beta_r^H(t-\varrho_1(t))} - \chi_s + \chi_0 + u_i(t), \\ {}_0^{\mathbb{C}}D_t^{\gamma}\beta_s(t) = -\phi_s\beta_s(t) - \hat{\omega}_s\alpha_s(t-\varrho_2(t)) + u_j(t), \end{cases} \tag{36}$$

where the parameters are the same system (35).

We will consider the following two cases:

Case 1. In Theorem 3.1 we choosing parameters $\eta_1 = 2.3$, $\eta_2 = 2.1$, $\eta_3 = 2.1$, $\mu_1 = 3.09$, $\mu_2 = 2.89$ and $\mu_3 = 2.97$ then, by solving the LMIs Eq. (10)–(13), it is can easy to see that

$$\Omega_1 = \begin{bmatrix} 0.6442 & 0.0024 & -0.0042 \\ 0.0024 & 0.6438 & -0.0030 \\ 0.0042 & -0.0030 & 0.6439 \end{bmatrix},$$

$$\Omega_2 = \begin{bmatrix} 0.7864 & 0.003 & -0.0005 \\ 0.0003 & 0.7835 & -0.0008 \\ -0.0005 & -0.0008 & 0.7839S \end{bmatrix},$$

and the controller gain matrices are

$$\Theta_1 = \begin{bmatrix} 0.7723 & 2.0506 & -2.4760 \\ -2.9134 & 2.0158 & 3.0323 \\ 3.3020 & -3.5077 & 0.6362 \end{bmatrix},$$

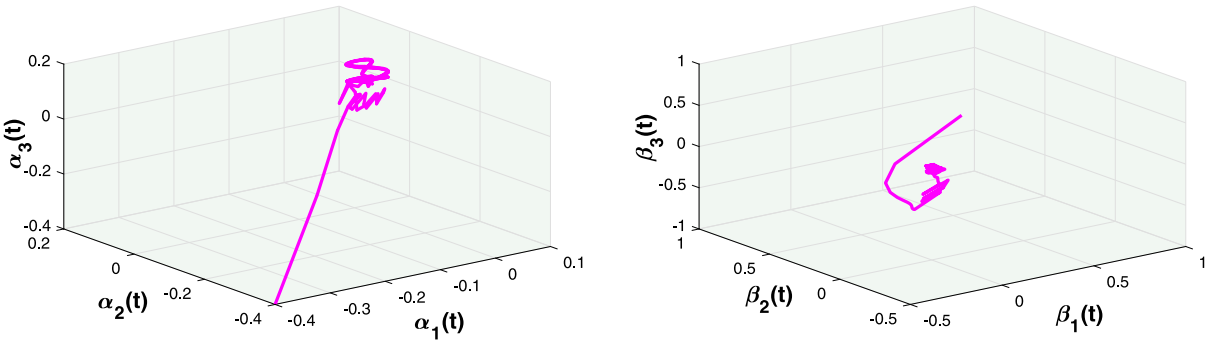

Fig. 4. Phase portrait of mRNA and protein levels of the FGRNs of repressilator model (35).

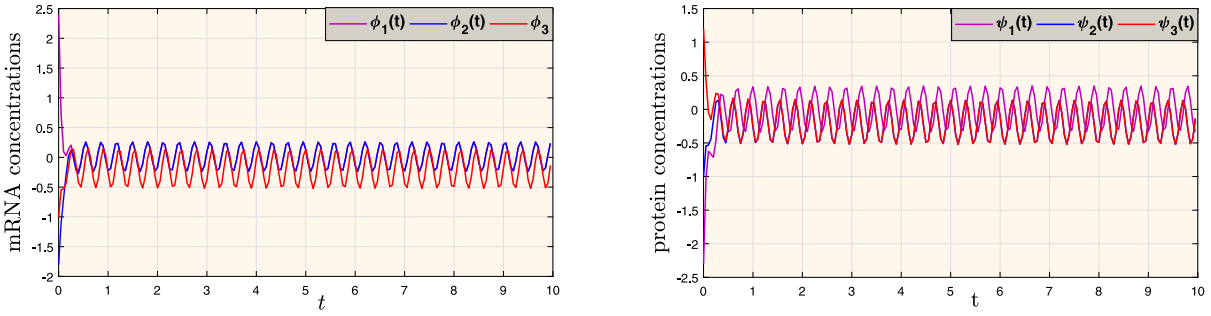

Fig. 5. Transient response of the mRNA and protein concentrations of system (36) without controller.

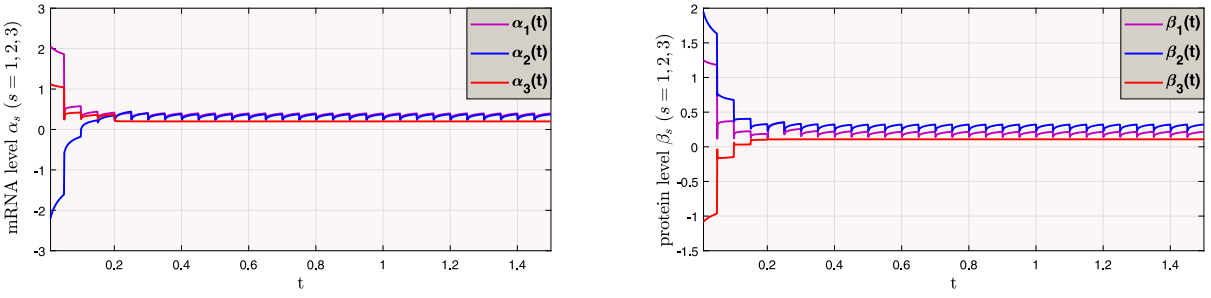

Fig. 6. Transient response of the mRNA and protein concentrations of system (36) with impulsive controller.

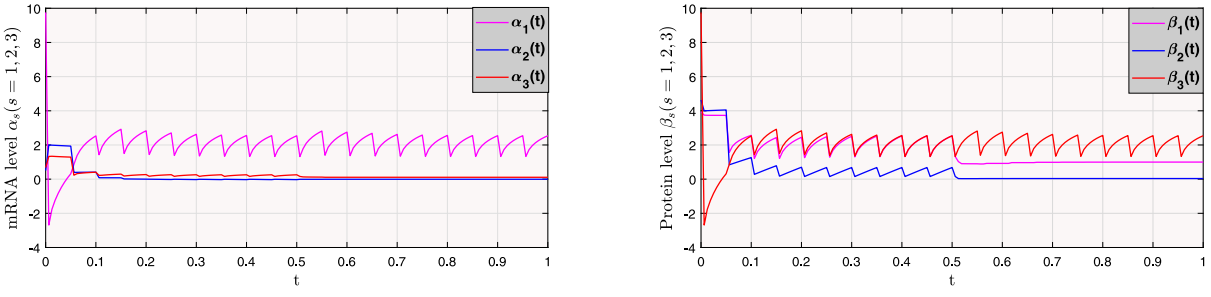

Fig. 7. Transient response of the mRNA and protein concentrations of system (36) with impulsive controller (time-varying delay-free case).

$$\Theta_2 = \begin{bmatrix} 3.3492 & 2.5563 & 3.9683 \\ 0.7406 & -0.8804 & 0.8814 \\ 0.2550 & -0.0909 & -1.0056 \end{bmatrix}$$

and the finite-time is about $t = 3.4$ according to the Eq. (13) at $\epsilon = 7.9$, $\delta = 3.1$. Therefore, the system (36) can achieve FTMLS under the designed controller (8). Under impulsive controller (8), the trajectories of the mRNA and protein concentration states $\alpha_s(t)$, and $\beta_s(t)$ $(s = 1, 2, 3)$ respectively are shown in Fig. 6. The time-varying delay-free case, the system (36) under impulsive control cannot be stable, which is shown in Fig. 7.

Case 2. From Theorem 3.6 we choosing parameters $\hat{\mu}_1 = 3.7$, $\hat{\mu}_2 = 3.9$, $\hat{\mu}_3 = 2.7$, $\eta_1 = 4.03$, $\eta_2 = 3.35$ and $\eta_3 = 3.76$ then, by solving the LMIs Eq. (25)–(28), it is can easy to see that

$$\Omega_1 = \begin{bmatrix} 0.0731 & 0.3070 & -0.1300 \\ 0.5238 & 0.7235 & -0.0200 \\ -0.1300 & -0.0200 & -0.8235 \end{bmatrix},$$

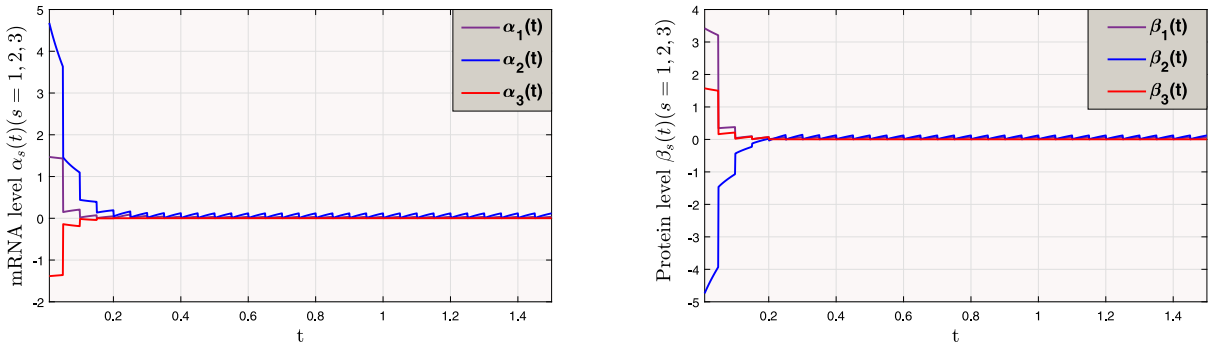

Fig. 8. Transient response of the mRNA and protein concentrations of system (36) with impulsive actuator saturation.

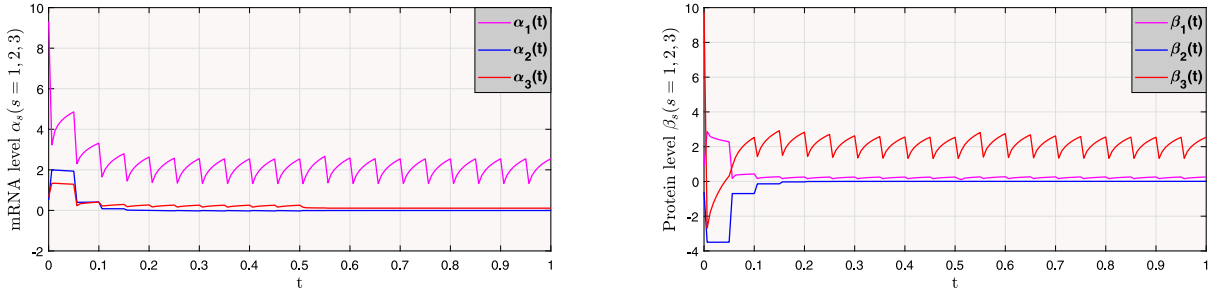

Fig. 9. Transient response of the mRNA and protein concentrations of system (36) with impulsive actuator saturation (time-varying delay-free case).

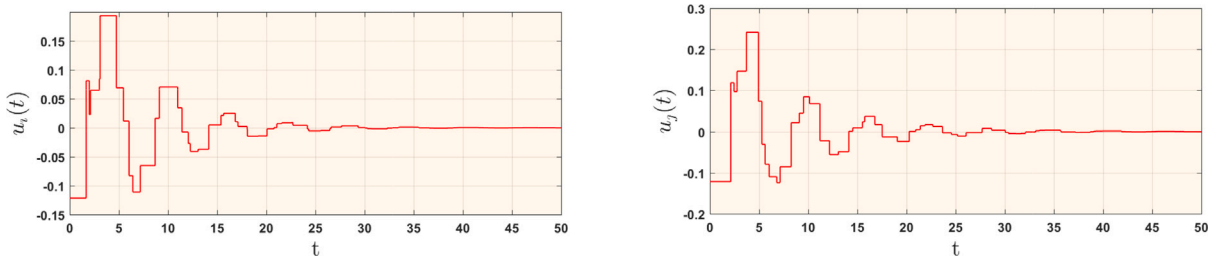

Fig. 10. Control signals of $u_i(t)$ and u_j in Eq. (8).

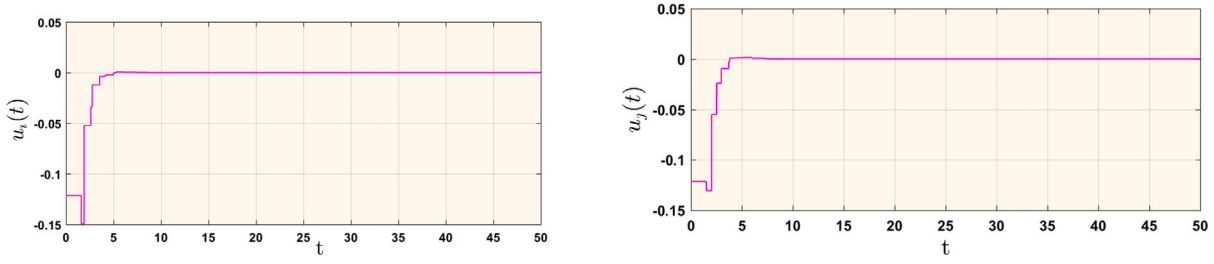

Fig. 11. Control signals of $u_i(t)$ and u_j in Eq. (20).

$$\Omega_2 = \begin{bmatrix} 0.3576 & 0.2000 & -0.4000 \\ 0.2000 & 0.4276 & -0.7000 \\ -0.4000 & -0.7000 & 0.8276 \end{bmatrix}.$$

and gain matrices

$$\Psi_1 = \begin{bmatrix} -0.9976 & 2.7709 \\ -0.8379 & -0.8043 \end{bmatrix}, \Psi_2 = \begin{bmatrix} -0.2387 & -0.3150 \\ -2.6684 & -2.0783 \end{bmatrix},$$

$$\Xi_1 = \begin{bmatrix} -0.1053 & 0.0705 \\ -0.0046 & -0.0007 \end{bmatrix}, \Xi_2 = \begin{bmatrix} -0.0015 & 0.1080 \\ -0.0164 & -0.0332 \end{bmatrix},$$

and the finite-time is about $t = 1.2$ according to the Eq. (29) at $\epsilon = 5.9$, $\delta = 2.5$. Therefore, the system (36) can achieve FTMLS under the designed controller (20). Fig. 8 depicts the impulsive actuator saturation controlled trajectories of $\alpha_s(t)$, $\beta_s(t)$ $(s = 1, 2, 3)$, which confirmed the feasibility and validity of the established theoretical results. Figs. 9 and 10 demonstrate the control signals for mRNA and protein concentrations, respectively. In addition, the time-varying delay-free case, the system (36) under impulsive control with actuator saturation cannot be stable, which is shown in Fig. 11. The Matlab simulation results for this example are shown in Figs. 4–11, and it can be observed that the proposed impulsive control and actuator saturation perform very well, confirming that the control system described in this study is effective for FTMLS of FGRNs. Furthermore, the time-varying delay is the main source of poor performance, oscillation and unstable of the system behaviors. For example, when the delay-free case, the system

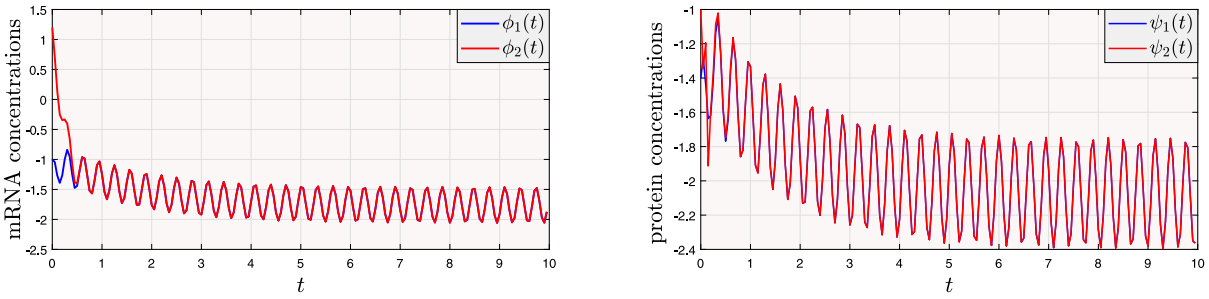

Fig. 12. Transient response of the mRNA and protein concentrations of system (6) without controller.

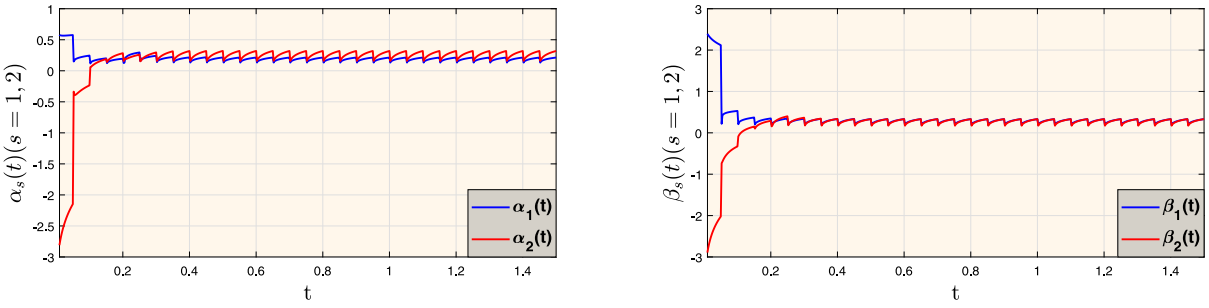

Fig. 13. Transient response of the mRNA and protein concentration of system (6) with impulsive controller (8).

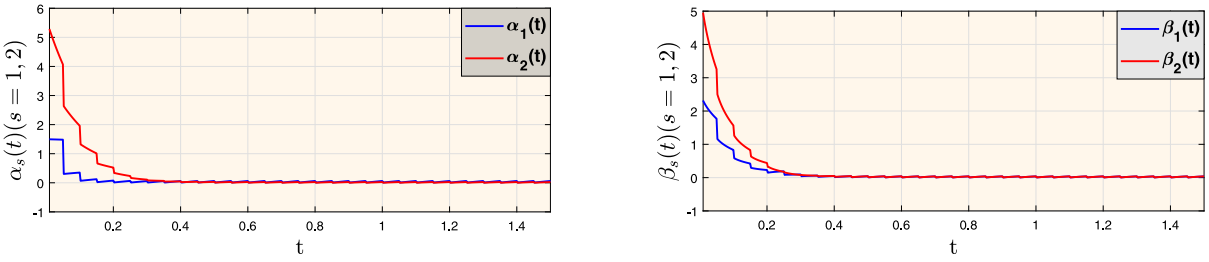

Fig. 14. Transient response of the mRNA and protein concentration of system (6) with impulsive control with actuator saturation (20).

(36) cannot be stable, which is shown in Figs. 6 and 10. The stabilizing impact of the time-varying delay in the system (36) is systematically considered.

Remark 4.1. It is mentioned that Example 4.1 includes FTMLS performance of system (36), which means that, the simulation study and obtained FTMLS criterion are more general than others on this subject (see [19–23]). More particularly, the existing works on this issue only focused on Mittag-Leffler stability (see [22]) and impulsive control (see [23]) performance, but the FTMLS criterion has been developed in this article unifies impulsive control and actuator saturation performances in a single work together with the improved techniques Lemma 2.5. Thus, the proposed technique and designed impulsive control and actuator saturation in this article generalize the other studies more effectively, which clearly shows the merits and novel contribution of this studies. In addition, the corresponding criteria of FTMLS are verified for the repressilator model by three repressor genes ($lacl$, $tetR$ and cl) whose data can be relatively changed as the parameters vary properly as [11]. Under the different parameters and control gain matrices, the obtained criteria in this article are really more diversity, higher flexibility, lower conservatism, and smaller computation than the ones in [11].

Example 4.2. Consider a class of fractional-order genetic regulatory networks system (6) with $s = 1, 2$; $r = 1, 2$; $\gamma = 0.93$, $\mathcal{P} = \begin{bmatrix} 3.1 & 0 \\ 0 & 2.9 \end{bmatrix}$, $\mathcal{W} = \begin{bmatrix} 2.4 & 0 \\ 0 & 3.5 \end{bmatrix}$, $\mathcal{Q} = \begin{bmatrix} 1.7 & 0 \\ 0 & 2.8 \end{bmatrix}$, $\mathcal{V} = \begin{bmatrix} 0 & 0 \\ -3.7 & 0 \end{bmatrix}$, $\varrho_1(t) = 3.13$, $\varrho_2(t) = 2.05$ and $\hbar(\beta) = \frac{\beta^2}{1+\beta^2}$. From the Assumption $(\mathcal{H}1)$ with $G_1 = 0$ and $G_2 = \text{diag}(0.5, 0.5)$. Now, we controller parameters values selected are as follows $\hat{\mu}_1 = 0.9$, $\hat{\mu}_2 = 1.3$, $\eta_1 = 0.9$ and $\eta_2 = 0.7$. From Theorem 3.6, we solve Eq. (25)–(28) and the feasible solutions are given by $\hat{\mu}_1 = 3.7$, $\hat{\mu}_2 = 3.9$, $\hat{\mu}_3 = 2.7$, $\eta_1 = 4.03$, $\eta_2 = 3.35$ and $\eta_3 = 3.76$, it is can easy to see that

$$\Omega_1 = \begin{bmatrix} 0.0731 & 0.3070 \\ 0.5238 & 0.7235 \end{bmatrix}, \Omega_2 = \begin{bmatrix} 0.3576 & 0.2000 \\ 0.2000 & 0.4276 \end{bmatrix}$$

and gain matrices

$$\Psi_1 = \begin{bmatrix} 0.9413 & -0.0235 & 0.0250 \\ -0.0235 & 0.9613 & -0.0386 \\ 0.0250 & -0.0397 & 0.8090 \end{bmatrix},$$

$$\Psi_2 = \begin{bmatrix} -0.1707 & 0.0002 & -0.0066 \\ -0.0003 & -0.0080 & 0.1602 \\ 0.1007 & -0.0003 & -0.2023 \end{bmatrix},$$

$$\Xi_1 = \begin{bmatrix} 0.2608 & 0.0008 & -0.2574 \\ -0.0006 & -0.2575 & 0.0004 \\ -0.1606 & -0.0880 & -0.0040 \end{bmatrix},$$

$$\Xi_2 = \begin{bmatrix} -0.0896 & -0.0004 & -0.0003 \\ -0.0002 & 0.0880 & 0.2603 \\ -0.0375 & -0.0397 & 0.0374 \end{bmatrix}.$$

Thus, the conditions in Theorem 3.6 are satisfied. So, the FGRNs system (6) are achieve the FTMLS via controller (20). Fig. 12 depicts the state trajectories of the mRNA and protein concentrations without the controller. Fig. 13 shows the simulation results for mRNA and protein concentrations of system (6) with impulsive control. The simulation results for mRNA and protein concentrations of system (6) with impulsive control and actuator saturation as shown in Fig. 14. The above simulation results have verified that the designed controller is effective for FTMLS of FGRNs under impulsive control and actuator saturation.

5. Conclusion

This article has investigated the saturated impulsive control scheme for the FTMLS problem of FGRNs. This article introduces a new established controller which involves saturated impulsive controller scheme is presented. Based on the fractional Lyapunov direct method, polytopic representation approach and a novel impulsive differential function inequality, LMI criteria are presented to ensure FTMLS of the considered model via impulsive control with actuator saturation. The concentrations of mRNAs and proteins were estimated using an impulsive control based on available network outputs, ensuring that the error system was finite-time stable. In order to display the effectiveness of the theoretical study, a mathematical model of the repressilator was exploited as a synthetic oscillatory network of transcriptional regulators in Escherichia coli [11] and their simulation diagrams live up to show our expectations and validity of the designed state estimator. In the near future, hybrid impulsive controller as well as other research topics such as Event-triggered control [34] and sampled-data control [13] of FGRNs under different communication protocols will be further investigated based on the methods proposed in this article.

CRediT authorship contribution statement

G. Narayanan: Conceptualization, Methodology. **M. Syed Ali:** Supervision. **Rajagopal Karthikeyan:** Software, Validation. **Grienggrai Rajchakit:** Data curation, Writing – original draft. **Anuwat Jirawattanapanit:** Visualization, Investigation.

Declaration of competing interest

The authors declare that they have no known competing financial interests or personal relationships that could have appeared to influence the work reported in this paper.

Data availability

No data was used for the research described in the article.

Acknowledgments

We thank the financial support from the National Research Council of Thailand (Talented Mid-Career Researchers) Grant Number N42A650250.

References

[1] V. Rani, R.S. Sengar, Biogenesis and mechanisms of microRNA-mediated gene regulation, Biotechnol. Bioeng. 119 (2022) 685–692.
[2] M. Ahmad, L.T. Jung, A. Bhuiyan, From DNA to protein: Why genetic code context of nucleotides for DNA signal processing? A review, Biomed. Signal Process. Control 34 (2017) 44–63.
[3] N. Padmaja, P. Balasubramaniam, Mixed H_∞/passivity based stability analysis of fractional-order gene regulatory networks with variable delays, Math. Comput. Simulation 192 (2022) 167–181.
[4] K. Su, N. Wang, Q. Shao, H. Liu, B. Zhao, S. Ma, The role of a ceRNA regulatory network based on lncRNA MALAT1 site in cancer progression, Biomed. Pharmacother. 137 (2021) 111389.
[5] S. Kilicarslan, M. Celik, S. Sahin, Hybrid models based on genetic algorithm and deep learning algorithms for nutritional Anemia disease classification, Biomed. Signal Process. Control 63 (2021) 102231.
[6] C. Cosentino, W. Curatola, M. Bansal, D. Bernardo, F. Amato, Piecewise affine approach to inferring cell cycle regulatory network in fission yeast, Biomed. Signal Process. Control 2 (2007) 208–216.
[7] G. Narayanan, M. Syed Ali, R. Karthikeyan, G. Rajchakit, A. Jirawattanapanit, Novel adaptive strategies for synchronization control mechanism in nonlinear dynamic fuzzy modeling of fractional-order genetic regulatory networks, Chaos Solitons Fractals 165 (2022) 112748.
[8] Y. Qin, J. Wang, X. Chen, K. Shi, H. Shen, Anti-disturbance synchronization of fuzzy genetic regulatory networks with reaction–diffusion, J. Franklin Inst. B 359 (2022) 3733–3748.
[9] H. Jiao, L. Zhang, Q. Shen, J. Zhu, P. Shi, Robust gene circuit control design for time-delayed genetic regulatory networks without SUM regulatory logic, IEEE/ACM Trans. Comput. Biol. Bioinform. 15 (2018) 2086–2093.
[10] V. Vembarasan, G. Nagamani, P. Balasubramaniam, J.H. Park, State estimation for delayed genetic regulatory networks based on passivity theory, Math. Biosci. 244 (2013) 165–175.
[11] K. Ratnavelu, M. Kalpana, P. Balasubramaniam, Stability analysis of fuzzy genetic regulatory networks with various time delays, Bull. Malays. Math. Sci. Soc. 41 (2018) 491–505.
[12] X. Li, R. Rakkiyappan, C. Pradeep, Robust μ-stability analysis of Markovian switching uncertain stochastic genetic regulatory networks with unbounded time-varying delays, Commun. Nonlinear Sci. Numer. Simul. 17 (2012) 3894–3905.
[13] M. Syed Ali, N. Gunasekaran, C.K. Ahn, P. Shi, Sampled-data stabilization for fuzzy genetic regulatory networks with leakage delays, IEEE/ACM Trans. Comput. Biol. Bioinform. 15 (2018) 271–285.
[14] H. Shen, Y. Men, J. Cao, J.H. Park, H_∞ Filtering for fuzzy jumping genetic regulatory networks with Round-Robin protocol: A hidden Markov model based approach, IEEE Trans. Fuzzy Syst. 28 (2020) 112–121.
[15] N. Jiang, X. Liu, W. Yu, J. Shen, Finite-time stochastic synchronization of genetic regulatory networks, Neurocomputing 167 (2015) 314–321.
[16] Z.H. Guan, D. Yue, B. Hu, T. Li, F. Liu, Cluster synchronization of coupled genetic regulatory networks with delays via aperiodically adaptive intermittent control, IEEE Trans. NanoBiosci. 16 (2017) 585–599.
[17] G. Narayanan, M. Syed Ali, G. Rajchakit, A. Jirawattanapanit, B. Priya, Stability analysis for Nabla discrete fractional-order of Glucose-insulin regulatory system on diabetes mellitus with Mittag-Leffler kernel, Biomed. Signal Process. Control 80 (2023) 104295.
[18] Y. Qiao, H. Yan, L. Duan, J. Miao, Finite-time synchronization of fractional-order gene regulatory networks with time delay, Neural Netw. 126 (2020) 1–10.
[19] Z. Zhang, J. Zhang, Z. Ai, A novel stability criterion of the time-lag fractional-order gene regulatory network system for stability analysis, Commun. Nonlinear Sci. Numer. Simul. 66 (2019) 96–108.
[20] C. Huang, J. Cao, M. Xiao, Hybrid control on bifurcation for a delayed fractional gene regulatory network, Chaos Solitons Fractals 87 (2016) 19–29.
[21] A. Pratap, R. Raja, R. Agarwal, J. Alzabut, M. Niezabitowski, E. Hincal, Further results on asymptotic and finite-time stability analysis of fractional-order time-delayed genetic regulatory networks, Neurocomputing 475 (2022) 26–37.
[22] F. Ren, F. Cao, J. Cao, Mittag-Leffler stability and generalized Mittag-Leffler stability of fractional-order gene regulatory networks, Neurocomputing 160 (2015) 185–190.
[23] T. Stamov, I. Stamov, Design of impulsive controllers and impulsive control strategy for the Mittag-Leffler stability behavior of fractional gene regulatory networks, Neurocomputing 424 (2021) 54–62.
[24] X. Li, D. Peng, J. Cao, Lyapunov stability for impulsive systems via event-triggered impulsive control, IEEE Trans. Automat. Control 65 (2020) 4908–4913.
[25] Q. Zhu, J. Cao, Stability analysis of Markovian jump stochastic BAM neural networks with impulse control and mixed time delays, IEEE Trans. Neural Netw. Learn. Syst. 23 (2012) 467–479.
[26] X. Li, S. Song, Research on synchronization of chaotic delayed neural networks with stochastic perturbation using impulsive control method, Commun. Nonlinear Sci. Numer. Simul. 19 (2014) 3892–3900.
[27] M. Luo, J. Jiao, R. Wang, Impulsive control of a nonlinear dynamical network and its application to biological networks, J. Biol. Phys. 45 (2019) 31–44.
[28] X. Tan, J. Cao, X. Li, Consensus of leader-following multi-agent systems: A distributed event-triggered impulsive control strategy, IEEE Trans. Cybern. 49 (2019) 792–801.
[29] I. Stamova, G. Stamov, Mittag-Leffler synchronization of fractional neural networks with time-varying delays and reaction–diffusion terms using impulsive and linear controllers, Neural Netw. 96 (2017) 22–32.
[30] S. Yang, C. Hu, J. Yu, H. Jiang, Exponential stability of fractional-order impulsive control systems with applications in synchronization, IEEE Trans. Cybern. 50 (2020) 3157–3168.
[31] X. Song, X. Li, C.K. Ahn, S. Song, Space-dividing-based cluster synchronization of reaction–diffusion genetic regulatory networks via intermittent control, IEEE Trans. NanoBiosci. 21 (2022) 55–64.

[32] H. Shen, Y. Men, J. Cao, J.H. Park, H_∞ Filtering for fuzzy jumping genetic regulatory networks with Round-Robin protocol: A hidden-Markov-model-based approach, IEEE Trans. Fuzzy Syst. 28 (2020) 112–121.
[33] L. Zhang, X. Zhang, Y. Xue, X. Zhang, New method to global exponential stability analysis for switched genetic regulatory networks with mixed delays, IEEE Trans. NanoBiosci. 19 (2020) 308–314.
[34] T. Yu, Y. Zhao, J. Wang, J. Liu, Event-triggered sliding mode control for switched genetic regulatory networks with persistent Dwell time, Nonlinear Anal. Hybrid Syst. 44 (2022) 101135.
[35] N. Yosef, A. Regev, Impulse control: Temporal dynamics in gene transcription, Cell 144 (2011) 886–896.
[36] G. Narayanan, M. Syed Ali, H. Alsulami, B. Ahmad, J.J. Trujillo, A hybrid impulsive and sampled-data control for fractional-order delayed reaction–diffusion system of mRNA and protein in regulatory mechanisms, Commun. Nonlinear Sci. Numer. Simul. 111 (2022) 106374.
[37] G. Ling, M.F. Ge, Y.H. Tong, Q. Fan, Exponential synchronization of delayed switching genetic oscillator networks via mode-dependent partial impulsive control, Neural Process. Lett. 53 (2021) 1845–1863.
[38] J. Qiu, K. Sun, C. Yang, X. Chen, X. Chen, A. Zhang, Finite-time stability of genetic regulatory networks with impulsive effects, Neurocomputing 219 (2017) 9–14.
[39] Z. He, C. Li, Y. Li, Z. Cao, X. Zhang, Local synchronization of nonlinear dynamical networks with hybrid impulsive saturation control inputs, Appl. Math. Comput. 410 (2021) 126452.
[40] D. Ouyang, J. Shao, H. Jiang, S.K. Nguang, H.T. Shen, Impulsive synchronization of coupled delayed neural networks with actuator saturation and its application to image encryption, Neural Netw. 128 (2020) 158–171.
[41] H. Li, C. Li, D. Ouyang, S.K. Nguang, Impulsive synchronization of unbounded delayed inertial neural networks with actuator saturation and sampled-data control and its application to image encryption, IEEE Trans. Neural Netw. Learn. Syst. 32 (2021) 1460–1473.
[42] Z. Li, J. Fang, T. Huang, Q. Miao, H. Wang, Impulsive synchronization of discrete-time networked oscillators with partial input saturation, Inform. Sci. 422 (2018) 531–541.